Supplementary Information

pH-responsive de-PEGylated nanoparticles based on triphenylphosphine-quercetin self-assemblies for mitochondria-targeted cancer therapy

Lei Xing [a, b, c, 1], Jin-Yuan Lyu [a, 1], Yue Yang [d, 1], Peng-Fei Cui [a], Liu-Qing Gu [a], Jian-Bin Qiao [a], Yu-Jing He [a], Tian-Qi Zhang [a], Minjie Sun [a], Jin-Jian Lu [e], Xiaojun Xu [a, *], Yu Liu [d, *], and Hu-Lin Jiang [a, b, c, *]

[a] *State Key Laboratory of Natural Medicines, Department of Pharmaceutics, China Pharmaceutical University, Nanjing 210009, China*

[b] *Jiangsu Key Laboratory of Druggability of Biopharmaceuticals, China Pharmaceutical University, Nanjing, 210009, China*

[c] *Jiangsu Key Laboratory of Drug Screening, China Pharmaceutical University, Nanjing 210009, China*

[d] *Department of Biochemistry, School of Life Science and Technology, China Pharmaceutical University, Nanjing 210009, China*

[e] *State Key Laboratory of Quality Research in Chinese Medicine, Institute of Chinese Medical Sciences, University of Macau, Macao, China*

[1] These authors contributed equally to this work.

* Correspondence to:

Professor H. L. Jiang, State Key Laboratory of Natural Medicines, China Pharmaceutical University, Nanjing 210009, China.

Tel: +86-25-83271027; Fax: +86-25-83271027; E-mail: jianghulin3@163.com

Professor Y. Liu, Department of Biochemistry, School of Life Science and Technology, China Pharmaceutical University, Nanjing 210009, China.

Tel: +86-25-83271543; Fax: +86-25-83271019; E-mail: liuyuyaoda@163.com

Associate Professor X. Xu, State Key Laboratory of Natural Medicines, China Pharmaceutical University, Nanjing 210009, China.

Tel: +86-25-83271382; Fax: +86-25-83271379; E-mail: xiaojunxu2000@163.com

Contents

1. Materials and methods

1.1 Materials

Quercetin (Que) was obtained from Nanjing Zelang Medical Technology Co., Ltd (Nanjing, Jiangsu, China). 4-Bromobutyl triphenylphosphonium bromide (TPP) was obtained from Alfa Aesar Co., Inc. (Ward Hill, MA, USA). α-(2-aminoethyl)-ω-methylpoly(ethylene glycol) (PEG, Mw = 2000 Da) was obtained from Xiamen Sinopeg Biotech Co., Ltd. (Xiamen, Fujian, China). Sodium borohydride ($NaBH_4$) was obtained from Sinopharm Chemical Reagent Co., Ltd. (Shanghai, China). 4-Formylphenylboronic acid (PBA), Coumarin 6 (C6)，cesium carbonate (Cs_2CO_3) and fluorescein (Flu) were both obtained from J&K Co., Ltd. (Beijing, China). For *in vitro* cytotoxicity experiment, TPP was replaced by TPP-COOH which was prepared as previously described. DiR was purchased from Beijing Fanbo biochemical Co., Ltd. (Beijing, China). All other chemicals and reagents in this investigation were obtained from commercial sources with analytical grade and used without further purification.

1.2 Cell culture

HeLa, HepG2, A549 and MCF-7 cells were cultured in RPMI 1640 (KeyGEN, Nanjing, China). The cell culture media were supplemented with 10 % fetal bovine serum (FBS), 100 μg/mL streptomycin and 100 U/mL penicillin. Cells were grown at 37 ^{o}C in a humidified 5 % CO_2 atmosphere.

1.3 Animals

Male ICR mice (18~22 g) were purchased from Qinglongshan breading farm (Nanjing, China). All animal experiments were carried out in compliance with China Pharmaceutical University Institutional Animal Care and Use Committee. To obtain the tumor xenograft model, approximately 1×10^7 of H22 cells were inoculated subcutaneously in the right armpit region of the mice.

2. Synthesis & Characterization

2.1 Synthesis of TPP-Que and TPP-Flu conjugates

Cs2CO3 (2 mmol) and borax (7.2 mmol) was added into a solution of Que (2 mmol) and TPP (2 mmol) in anhydrous N, N-dimethylformamide (10 mL). The suspension

was then heated to 60 oC under an atmosphere of argon overnight. After cooling to room temperature, the reaction mixture was diluted with dichloromethane (DCM) and filtered off the solid. The filtrate was washed five times with 3 M HCl solution. The organic layer was dried over magnesium sulfate and concentrated under vacuum. And then the crude product was dissolved in proper amount of DCM and precipitated from rapidly stirred diethyl ether for 3 times. The solvents were decanted after each precipitation. Yellow powder was obtained after removing the residual solvent under vacuum distillation.1-3 The crude product was further purified by preparative thin layer chromatography [$CHCl_3$-MeOH (97:3)] to give a yellow solid. TPP-Flu was synthesized to study the subcellular localization of nanoparticles by the method described above.[4] ^{1}H-NMR spectrum of TPP-Que (1) (300 MHz, DMSO-d6): δ (ppm) = 1.59-2.11 (m, 4H, -CH_2×2), 3.98-4.34 (m, 4H, -CH_2×2), 6.33 (s, 1H, 6-H), 6.69 (s, 1H, 8-H), 6.88 (s, 1H, 5'-H), 7.53 (s, 1H, 6'-H), 7.65-7.98 (m, 16H, 15H = PPh3, 1H = 2'-H). ^{13}C-NMR spectrum of TPP-Que (300 MHz, DMSO-d6): δ (ppm) = 175.88(C4), 164.09(C7), 160.34(C5), 156.01(C9), 147.79(C4'), 147.23(C2), 145.04(C3'), 135.96(C3), 134.9(Ph), 133.61(Ph), 130.29(Ph), 121.86(C1'), 119.95(C6'), 118.81(Ph), 115.53(C2'), 115.27(C5'), 103.95(C10), 97.72(C6), 92.32(C8), 67.32[CH_2, $(CH_3CH_2)_2O$], 29.60(CH_2), 8.22[CH_3, $(CH_3CH_2)_2O$]. HRMS for TPP-Que (1) $[M-Br]^+$ 619.2. HRMS for TF (3) $[M-Br]^+$ 549.2.

2.2 Synthesis of PBA-PEG

PEG (0.25 mmol) and PBA (0.25 mmol) were dissolved in 10 mL anhydrous ethanol. Then two drops of acetic acid were added as the catalyst. The mixture was heated to 90 ^{o}C and refluxed for 24 h. After cooling to room temperature, $NaBH_4$ (1.25 mmol) was added in batches and reacted overnight.[5,6] Subsequently the reaction mixture was dried by vacuum distillation and then redissolved in distilled water. After dialyzed using a dialysis bag (MWCO= 500, Baomanbio, Shanghai, China) against distilled water for 48 h, flocculent white solid was obtained after lyophilization. ^{1}H-NMR spectrum of PBA-PEG (2) (300 MHz, DMSO-d6): δ (ppm) = 10 (s, 1H, -CHO), δ (ppm) = 7.5-8.5 (m, 6H, -$PhBO_2H_2$), δ (ppm) = 3.2-3.5 (m,

180H, -CH_2CH_2O-). HRMS for PEG: 2174.3 and HRMS for PBA-PEG (2): 2305.3.

2.3 Characterization of self-assembly behavior of TPP-Que

The critical aggregation concentration (CAC) of TPP-Que was measured by using pyrene as a fluorescence probe. Thirty μL pyrene solution (1×10^{-10} M in acetone) were added to 15 mL vials, and the solvent was removed by natural evaporation. Subsequently, 5 mL TPP-Que aqueous solutions of concentrations ranging from 10^{-5} to 1 mg/mL were added into the flasks. After 5 min ultrasonic treatment and stayed overnight, the emission spectra of the solutions were measured by spectrofluorophotometer (RF-5301, SHIMADZU, Japan).[7]

The formation mechanism of TQ NPs was investigated by adding Tween 20, Triton X-100, urea and NaCl to the TQ NPs solutions. Changes of diameter were recorded by dynamic light scattering (DLS, 90PlusZeta, Brookhaven, USA).[8]

2.4 pH-responsive de-PEGylation

The pH-responsive cleavage of the coordination bond was characterized by ^{1}H-NMR. Firstly, Que and PBA-PEG were separately dissolved in DMSO-d_6 at a concentration of about 170 mM. Then the two solutions were mixed to obtain a stock solution of Que-PBA-PEG conjugate at a concentration of 85 mM. Solutions of PBS at various pH values (pH 7.4, 6.6, and 5.5) were used to dilute the Que-PBA-PEG conjugate stock solution to 8.5 mM. Phosphate buffered saline (PBS) solutions were prepared according to Chinese Pharmacopoeia with D_2O as the solvent. These solutions were allowed to stand for an hour before high speed centrifugation, and then the supernatants were photographed and analyzed by ^{1}H-NMR (BRUKER AV-500, Switzerland).[9]

2.5 Preparation of TQ and TQ-PEG nanoparticles

In brief, 10 mg TPP-Que was completely dissolved in 100 μL anhydrous ethanol. Then, the solution was dropped into 5 mL of deionized water (pH = 10.5) and stirred for 30 min. After dialyzed in water for 12 h, TQ NPs were obtained. The preparation method of TQ-PEG NPs was the same as TQ NPs except the addition of 20 % molar ratio PBA-PEG in ethanol solution of TPP-Que.

C6 loaded TQ and TQ-PEG nanoparticles were prepared using the same

method. Briefly, 10 mg TQ was dissolved in 100 μL DMSO solution of C6 (230 μg/mL) and was dropped into 5 mL of deionized water (pH = 10.5) and stirred for 30 min. After dialyzed in water for 6 h, C6/TQ NPs were obtained. The preparation method of C6/TQ-PEG NPs (pH7.4) was the same as TQ NPs except the addition of 20 % molar ratio PBA-PEG in DMSO solution of TPP-Que. C6/TQ-PEG NPs in pH 6.5 was prepared by adjusting the pH of C6/TQ-PEG NPs solution using 0.01M HCL.

3. *In vitro* assay protocols

3.1 Subcellular localization

The localization of TPP-Flu nanoparticles (TF NPs) on HeLa cells was visualized by labeling the cells with MitoTracker Red (Invitrogen, USA) and observed by CLSM. HeLa cells were seeded at a density of 1×10^5 cells per well in a 35 mm glass bottom culture dish at 37 ^oC for 24 h. After being incubated with TF NPs for 18 h, the cells were washed by ice-cold PBS twice and then stained with 100 nM MitoTracker Red at 37 ^oC for 30 min. Subsequently the cells were fixed with 4 % paraformaldehyde, and then washed twice with PBS and observed by CLSM.

3.2 Cellular uptake of nanoparticles by HeLa cells

The cellular uptakes of the C6/TQ NPs, C6/TQ-PEG NPs and dePEGylation of C6/TQ-PEG NPs in the pH 6.5 were studied in HeLa cells using flow cytometry. HeLa cells (1×10^5/well) were seeded in 24-well plates with 1 mL of RPMI 1640 containing 10 % FBS, and incubated at 37 ^oC for 24 h. Then the media were replaced with serum-free media containing C6/TQ NPs, C6/TQ-PEG NPs and dePEGylation of C6/TQ-PEG NPs in the pH 6.5. After incubation for 1 h, 2 h and 4 h, Thereafter, culture media were removed and cells were washed with PBS for three times and treated with trypsin. A total of 1×10^4 cells were immediately analysed by FACS.

3.3 Cytotoxicity

The cytotoxicity was evaluated by 3-(4, 5-dimethylthiazol-2-yl)-2, 5-diphenyltetrazolium bromide (MTT) assay to HeLa, HepG2, A549 and MCF-7 cells.

Cells were seeded at a density of 0.8 × 10^4 cells per well in 200 μL of growth medium in 96-well plates and attached for 24 h according to previous reported method.[10,11] Then they were treated with different concentrations of PBA-PEG, TPP-COOH, Que (dissolved in complete media containing 1 % DMSO), TF NPs, TQ NPs, and TQ-PEG NPs. It should be noted that TPP-COOH was used to exclude toxicity derived from the alkyl bromide on TPP. Untreated cells and cells treated with 1 % DMSO were used as blank controls. After 48 h, the media were removed, washed twice with PBS and then replaced with 120 μL MTT fresh culture media solution (0.5 mg/mL). The cells were incubated for an additional 4 h at 37 °C. Then, the medium was removed and 150 μL DMSO was added to dissolve the formazan crystal formed by living cells. The absorbance at 490 nm of the solution in each well was recorded using a Microplate Reader (Thermo, USA).[12] All experiments were conducted in triplicate.

3.4 Cell apoptosis

HeLa cells cultures in 6-well plate were treated with Que, TQ NPs and TQ-PEG NPs at the same concentration of 20 μM for 24 h. Cells without treatments were used as a control. For quantitative measurement of apoptosis, treated cells were harvested and washed twice with ice-cold PBS. After stained with Annexin V-FITC/ propidium iodide (PI) Apoptosis Detection Kit (KeyGEN, Nanjing, China) in dark, these samples were analyzed by Fluorescence Activated Cell Sorting (FACS), and 1 × 10^4 events per sample were counted. The apoptosis rate was denoted as the percentage of Annexin V-FITC positive cells.

3.5 Activation of the mitochondria apoptosis pathway

3.5.1 Mitochondrial depolarization

HeLa cells cultures in 12-well plate were treated with Que, TQ NPs and TQ-PEG NPs at the same concentration of 20 μM for 24 h. Cells without treatments were used as a control. Subsequently the cells were trypsinized and resuspended in PBS. After incubated in 5 mM cationic lipophilic fluorochrome rhodamine 123 (KeyGEN, Nanjing, China) for 1 h at 37 °C in the dark，the cells were washed twice with ice-cold PBS and immediately analyzed by FACS.

3.5.2 Release of cytochrome *c* from mitochondria

HeLa cells were seeded in 6-well plates at a density of 2.0×10^5 cells per well and allowed to attach for 24 h. The cells were treated with Que, TQ NPs and TQ-PEG NPs at the same concentration of 20 μM for 24 h. Cells without treatments were used as a control. Cytosol and mitochondrial proteins were separately extracted using a cell mitochondria isolation kit (Beyotime, China) after treatments. The contents of cytochrome *c* (Cyt *c*) protein in cytosol and mitochondrial fractions were determined using a Human Cytochrome *c* ELISA Kit (Cusabio Biotech, Wuhan, China). The result was finally expressed as the content ratio of Cyt *c* in cytosol and mitochondria.

3.5.3 Activation of caspase-9 and caspase-3

HeLa cells were seeded in 6-well plates at a density of 2.0×10^5 cells per well and allowed to attach for 24 h. The cells were treated with different formulations at the same concentration of 20 μM for 24 h. Cells without treatments were used as a control. Caspase-9 and caspase-3 activities were determined using caspase-9 and caspase-3 activity kit (Beyotime, China), respectively. According to the manufacturer's protocol, treated cells were harvested and then washed with ice-cold PBS. After being lysed with lysis buffer (100 μL per 2×10^6 cells) for 15 min on ice, supernatant was collected to quantify the protein content by using a Bradford protein assay kit (KeyGEN, Nanjing, China). After mixing 40 μL of reaction buffer and 50 μL of sample solution, 10 μL of 2 mM caspase-9 and caspase-3 substrate were added in 96-well plates, respectively. After incubated at 37 ^{o}C for 3 h, caspase-9 and caspase-3 activities were quantified with a microplate spectrophotometer (Thermo, USA) at an absorbance of 405 nm. Caspase-9 and caspase-3 activities were further normalized by the protein content in each sample, respectively. The results were expressed as the fold of enzyme activity compared to that of controlled cells.

3.5.4 Measurement of ROS level

The intracellular level of ROS was detected using an oxidation-sensitive probe 2', 7'-dichlorfluorescin diacetate (DCFH-DA). Five μM DCFH-DA solutions were

loaded onto the cells at 37 ^{o}C for 20 min in the dark before drug treatments. Subsequently, various formulations were added and incubated at 37 ^{o}C. After washed twice with PBS, the treated cells were harvested and analyzed by FACS immediately.

3.6 Biodistribution

To evaluate the tumor targeting capacity of TQ-PEG NPs, mice models were randomly divided into two groups when the tumor volume reached about 500 mm^3. DiR labeled nanoparticles and free DiR were intravenously administrated via the tail vein at a DiR dose of about 0.25 mg/kg. At prearranged time intervals after injection, NIR fluorescent images were captured by *in vivo* imaging system (FX PRO, Kodak, USA). The mice were then sacrificed and the heart, livers, lungs, spleen, kidneys and tumor of every mouse were collected.

3.7 Antitumor efficacy *in vivo*

Antitumor efficacy *in vivo* was evaluated on H22 tumor-bearing mice when the tumor volume reached approximately 50 mm^3. The mice were weighed and randomly divided into four groups (n=4): (i) control group (5 % glucose solution); (ii) free doxorubicin at 2 mg/kg; (iii) free Que at 4 mg/kg (i.p. Que 5 mg/kg); (iv) TQ-PEG NPs at 4 mg/kg. Each group was injected intravenously via the tail vein except the free Que by intraperitoneal injection because of the insolubility of Que. The mice were administrated twice a week over a 14-day therapeutic period. Body weights were measured before administrations. At day 14, the mice were all sacrificed and dissected. Tumor tissues were collected and weighed.

3.8 Preliminary evaluation of the toxicity of TQ-PEG NPs

To evaluate the toxicity of different formulations to normal tissues, the heart, livers, kidneys, spleen and lungs of every mouse were excised and fixed in 10 % neutral buffered formalin for further H&E staining. Blood samples were also collected and centrifuged at 3000 rpm for 10 min to obtain serum for blood biochemical analysis, including the level of blood urea nitrogen (BUN) and creatinine (CR), lactate dehydrogenase (LDH), aspartate aminotransferase (AST) andalanine aminotransferase (ALT), which reflect the damage of kidney, heart and

liver, respectively.

3.9 Statistical analysis

Data are given as mean ± standard deviation. Statistical significance was tested by two-tailed Student's t-test or one-way ANOVA. Statistical significance was set at *$P < 0.05$, and extreme significance was set at **$P < 0.01$.

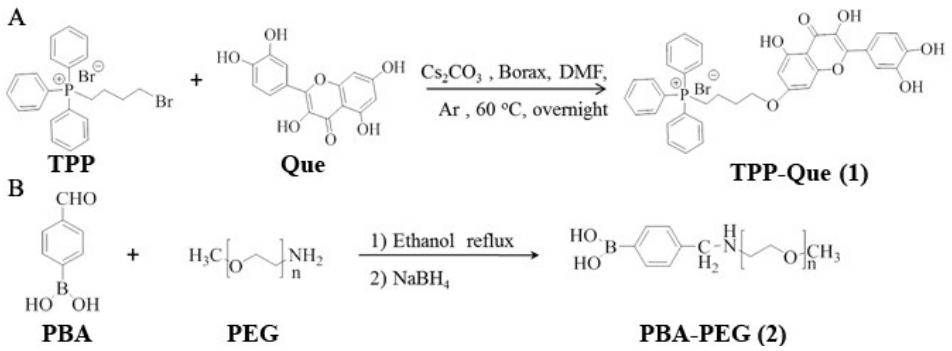

Fig. S1 Synthesis route of TPP-Que (A) and PBA-PEG (B).

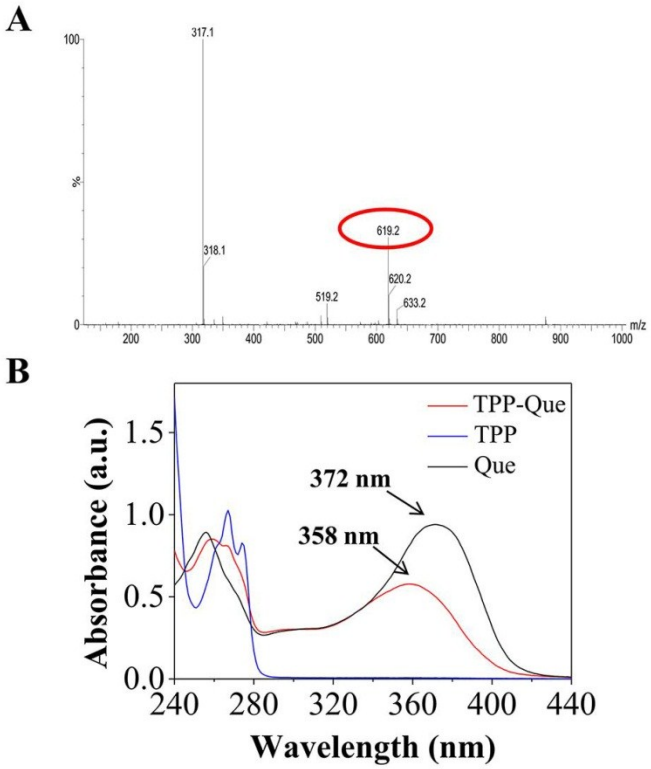

Fig. S2 Characterization of TPP-Que conjugates. (A) Mass spectrum analysis of TPP-Que conjugates showed the molecular ion peak was found at m/z 619.2. (B) UV-Vis spectra of TPP-Que, TPP and Que in methanol. The characteristic absorption band of Que was shifted from 372 nm to 358 nm after conjugated with TPP. This blue shift was used as a confirmation of the linkage between Que and TPP. [13]

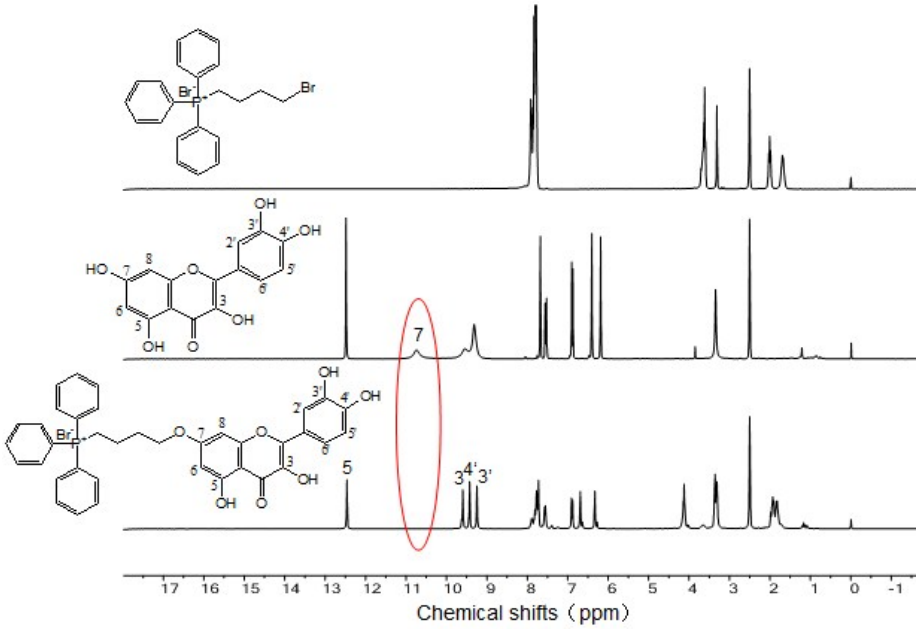

Fig. S3 ^{1}H-NMR spectra of TPP-Que, TPP and Que dissolved in DMSO-d_6.

Table S1 Chemical shifts (δ) of the aromatic protons of Que and TPP-Que measured in DMSO-d_6. Chemical shift differences (Δδ) relative to Que are shown in parentheses.

Compound	δ**(H-6)**	δ**(H-8)**	δ**(H-5')**	δ**(H-6')**
Que	6.18	6.38	6.87	7.53
TPP-Que	6.33(+0.15)	6.69(+0.31)	6.88(+0.01)	7.53(+0.00)

More importantly, the 7-H in the ^{1}H NMR spectrum of TPP-Que disappeared. Moreover, the chemical shift differences (Δδ) relative to Que (especially H-6 and H-8) are shown in Table S1. So the ^{1}H NMR spectrum of TPP-Que can demonstrate the TPP conjugated 7-position in Que (Fig. S3 and Table S1).

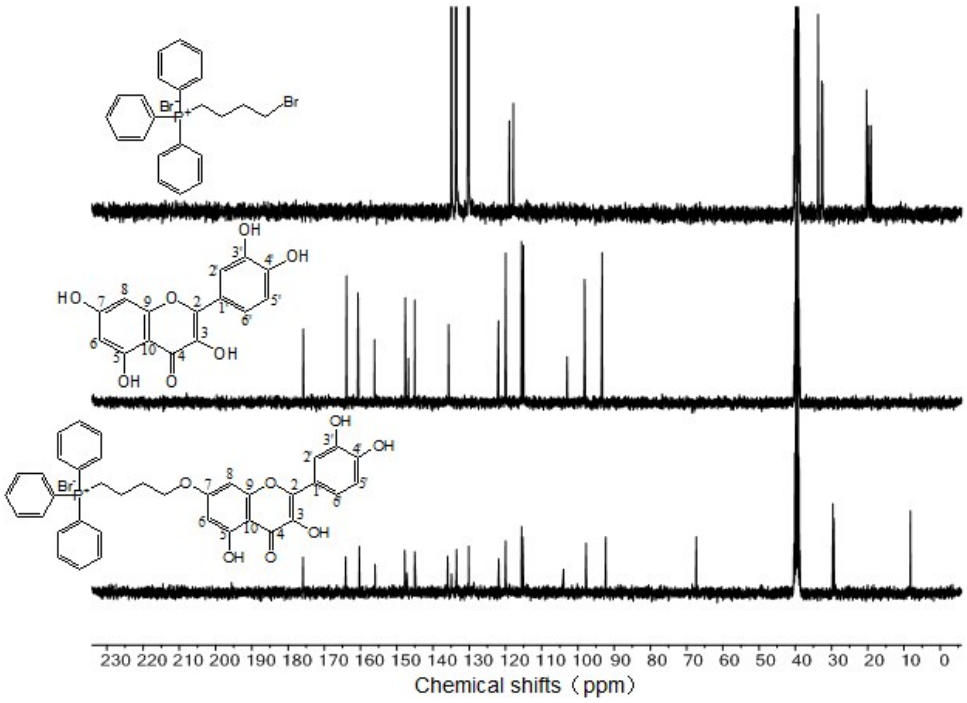

Fig. S4 ^{13}C-NMR spectra of TPP-Que, TPP and Que dissolved in DMSO-d_6.

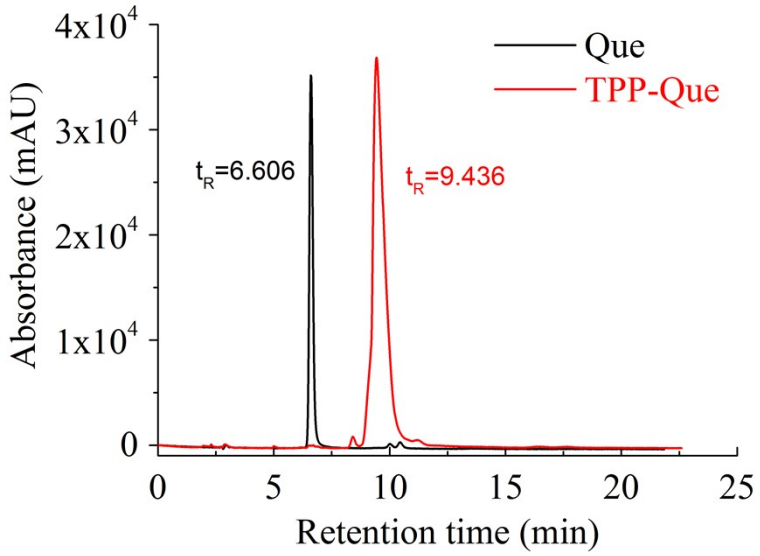

Fig. S5 HPLC spectra of TPP-Que and Que. Chromatographic conditions: C_{18} reversed-phase column (250 mm × 4.6 mm) packed with 5 μm diameter particles. Mobile phase: acetonitrile-water（40 : 60, v/v）containing 0.12 % acetic acid. Detection wavelength: 360nm. Column temperature: 25 °C. Flow rate: 1.0 ml/min. injection volume: l0 μL. TPP-Que (Content: 97.55 %，t_R = 9.436 min), Que (Content: 96.01 %，t_R = 6.606 min).

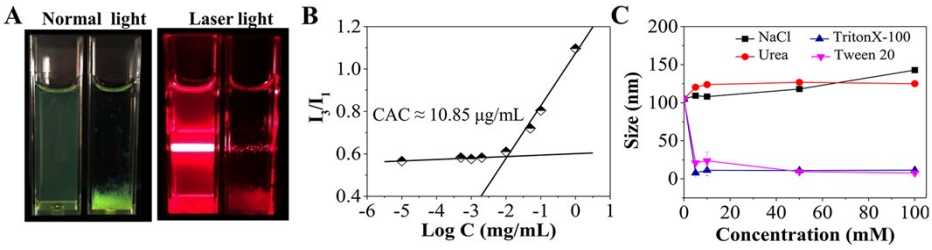

Fig. S6 Self-assembly behavior of TPP-Que conjugates. (A) The view of TQ NPs and Que precipitates under normal light and laser light. (B) Relationship between the fluorescent intensity ratio (I_3/I_1) of pyrene and TPP-Que concentration in water. (C) Aggregation mechanism of TPP-Que. The data are presented as average ± standard error (n= 3).

Fig. S6A showed that a clear Tyndall effect was observed in TPP-Que aqueous solution, which indicated the existence of abundant nanoparticles. While yellow precipitate of Que appeared in aqueous solution because of its insolubility. In the TPP-Que molecule, Que is hydrophobic and TPP is relatively hydrophilic, although TPP is known as a lipophilic cation. Owing to the amphiphilicity of TPP-Que, Que and TPP serve as essential components in the nanocarrier construction as well as the roles of drug and mitochondrial targeting moiety.

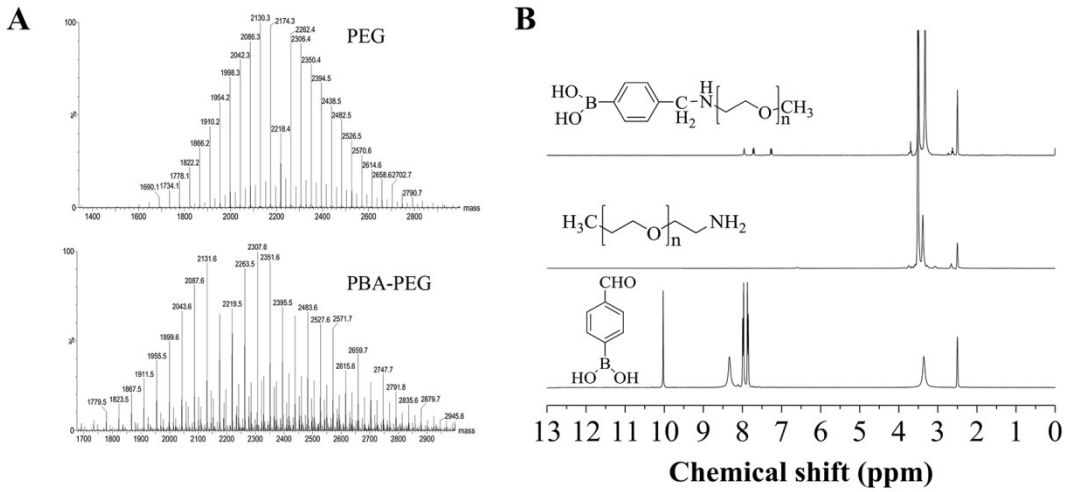

Fig. S7 Characterization of PBA-PEG. (A) Mass spectrum analysis of PEG and PBA-PEG found the average molecular weight at 2174.3 and 2305.3. (B) ^{1}H-NMR spectra of PEG-PBA, PEG and PBA dissolved in DMSO-d_6.

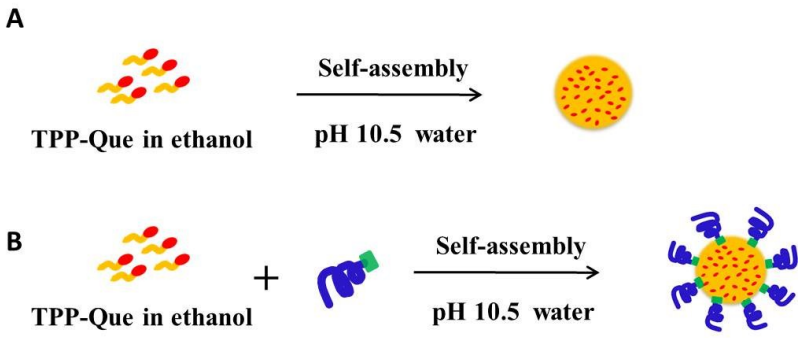

Scheme S1 Schematic illustration of the formation process of TQ NPs (A) and TQ-PEG NPs (B).

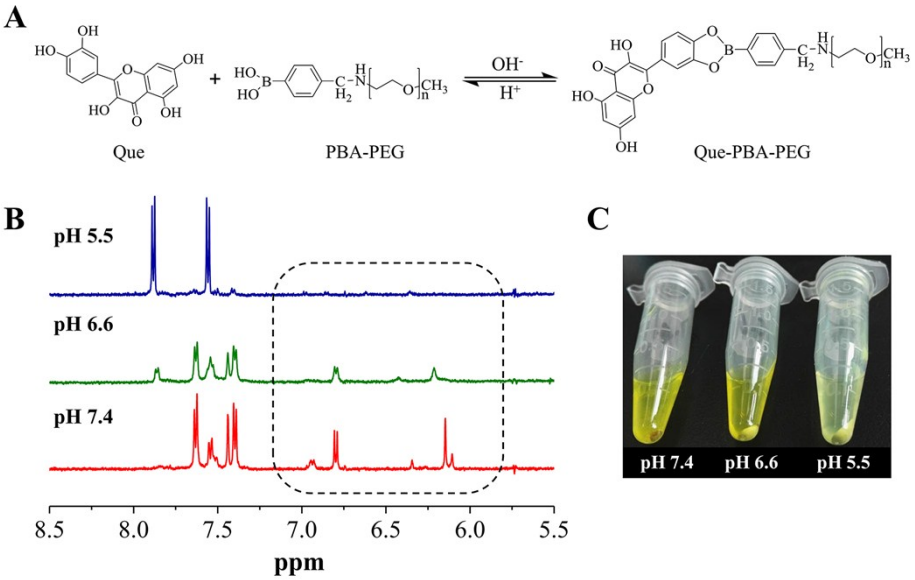

Fig. S8 pH-responsive interactions between Que and PBA-PEG. (A) Stable conjugate is formed at neutral and alkaline pH, while Que dissociates from Que-PBA-PEG in acidic environments. (B) pH-responsive cleavage of coordination bond characterized by ^{1}H-NMR. The dashed rectangle highlights the H signals derived from Que. (C) The photograph of samples in PBS solution of different pH.

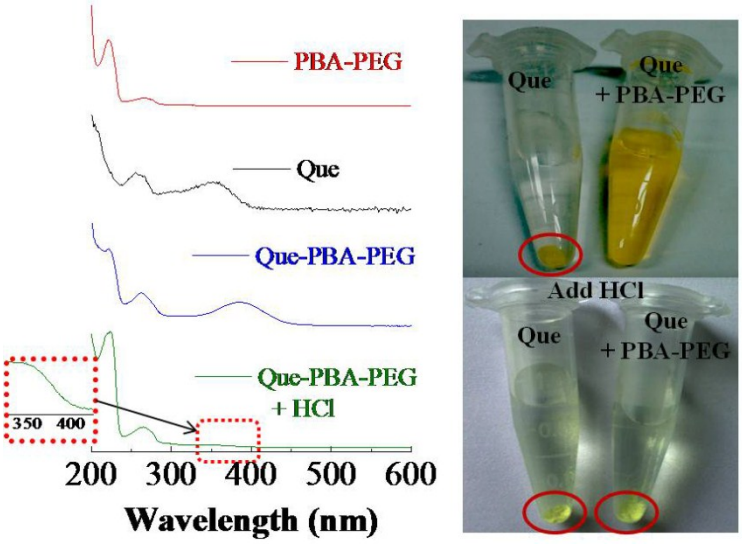

Fig. S9 Investigation of the interaction between Quercetin and PBA-PEG characterized by UV-vis spectra. Que existed as precipitate in pH 7.4 PBS solution. While yellow solution formed after the addition of PBA-PEG because of the formation of coordination bond between Que and PBA.

Que exists as insoluble light yellow powder in water, while Que-PBA-PEG conjugate can form yellow aqueous solution. Based on the difference of solubility, Que was used to take the place of TPP-Que. Que and PBA-PEG were mixed in deuterated PBS solution of pH values from 7.4 to 5.5. When the pH decreased to about 5.0, Que will immediately dissociate from Que-PBA-PEG conjugate, thus resulting in solution color fading and precipitate formation. By comparing the Que content in supernatants and the amount of precipitates in the resulting solutions, the relative cleavage degree of the coordination bonds can be characterized by ^{1}H-NMR. As shown in Fig. S8B, as the pH decreased from 7.4 to 5.5, the intensity of the H signals on Que decreased, and the yellow color of supernatant became lighter and precipitate of Que immediately increased (Fig. S8C), which illustrating the abscission of Que. Moreover, the signal intensity of peaks around 7.4 and 7.7 ppm were decreased and the peaks at 7.6 and 7.8 ppm increased. These results together with the changes on UV-vis spectra (Fig. S9) demonstrated the pH-responsive cleavage of the coordination bond from pH 7.4 to 5.5.

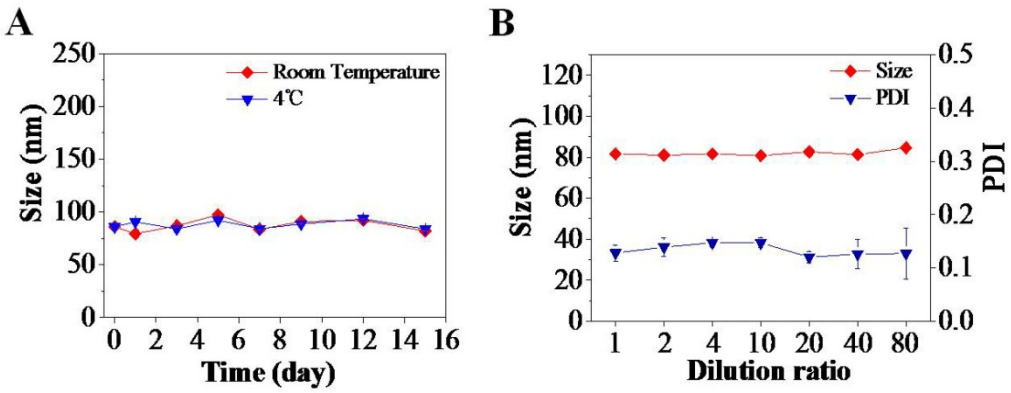

Fig. S10 Stability of TQ NPs. (A) Diameter fluctuation of TQ NPs at RT and 4 °C. (B) Integrity of TQ NPs in dilution. 2 mg/mL TQ NPs solution was diluted with water into various concentrations, and the diameter and PDI were measured by DLS. The data are presented as average ± standard error (n= 3).

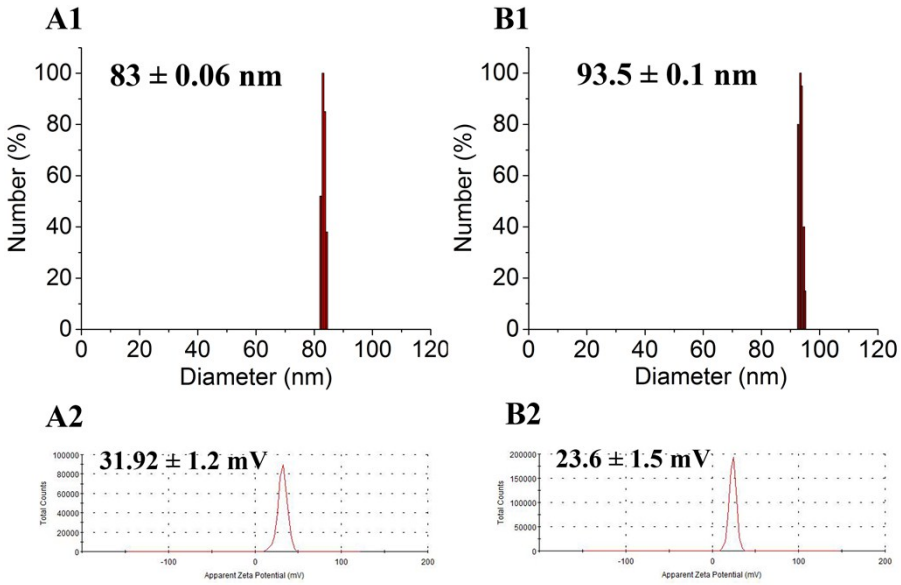

Fig. S11 Sizes (1) and Zeta potentials (2) of TQ NPs (A) and TQ-PEG NPs (B).

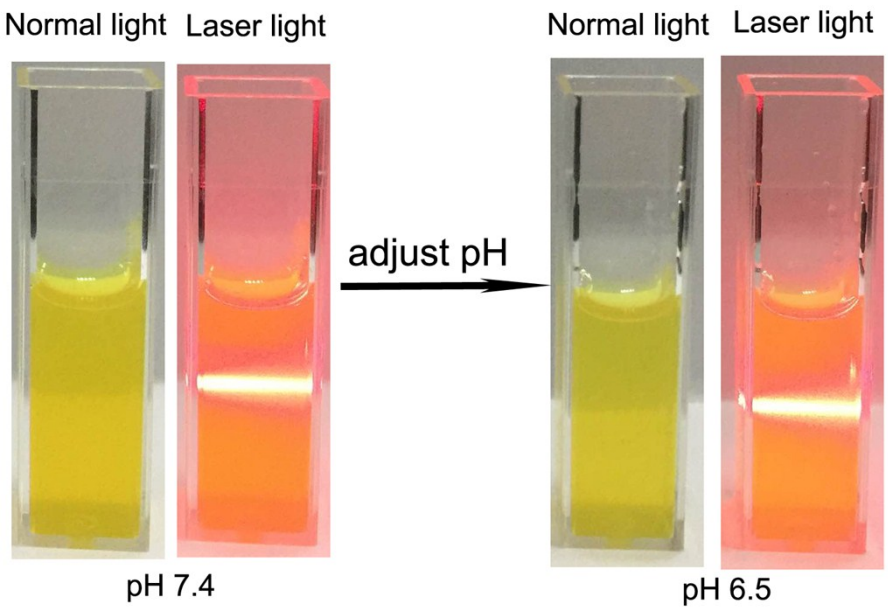

Fig. S12 The view of TQ-PEG NPs in the pH7.4 and pH 6.5 under normal light and laser light.

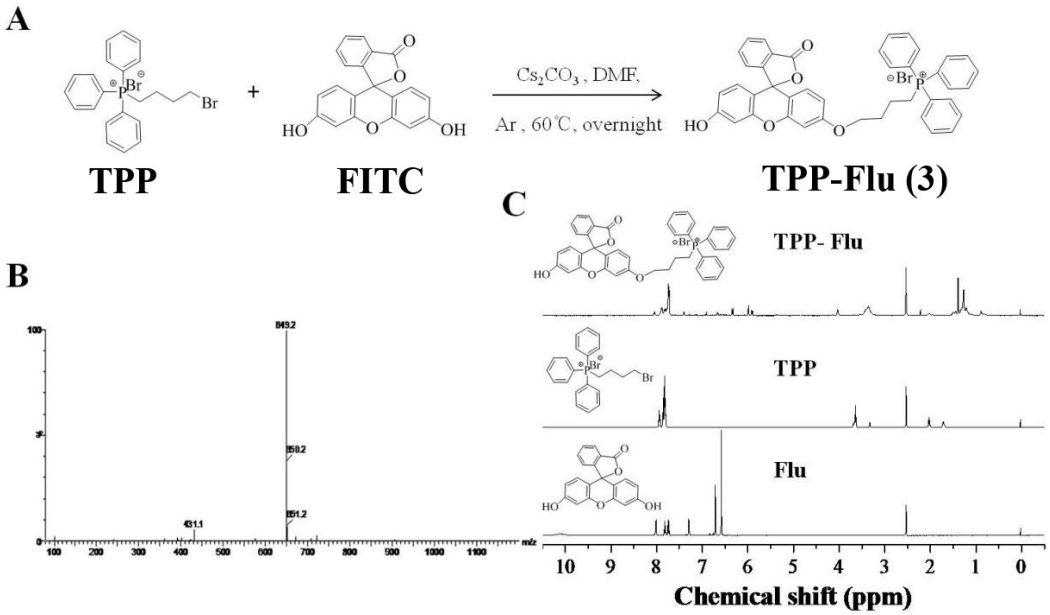

Fig. S13 (A) Synthesis route of TPP-Flu conjugate. (B) Mass spectrum analyze showed a molecular ion peak at m/z 549. (C) ^{1}H-NMR spectra of TPP-Flu, TPP, Flu dissolved in DMSO-d_6.

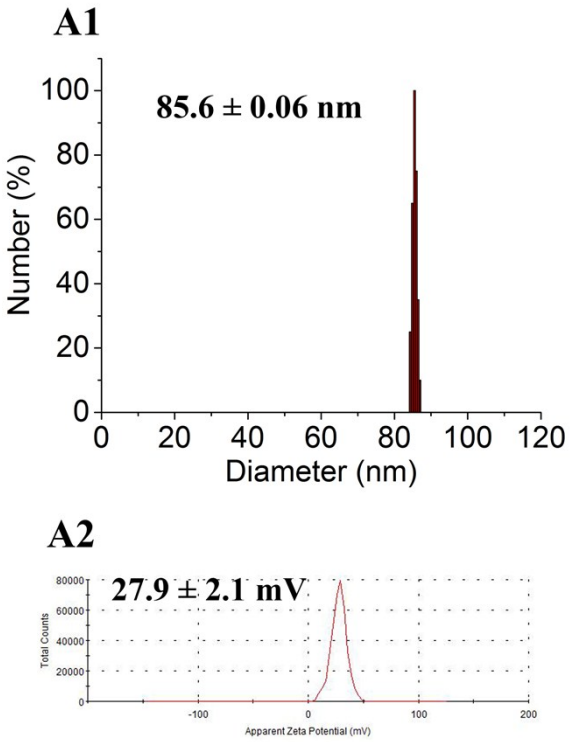

Fig. S14 Size (1) and Zeta potential (2) of TF NPs.

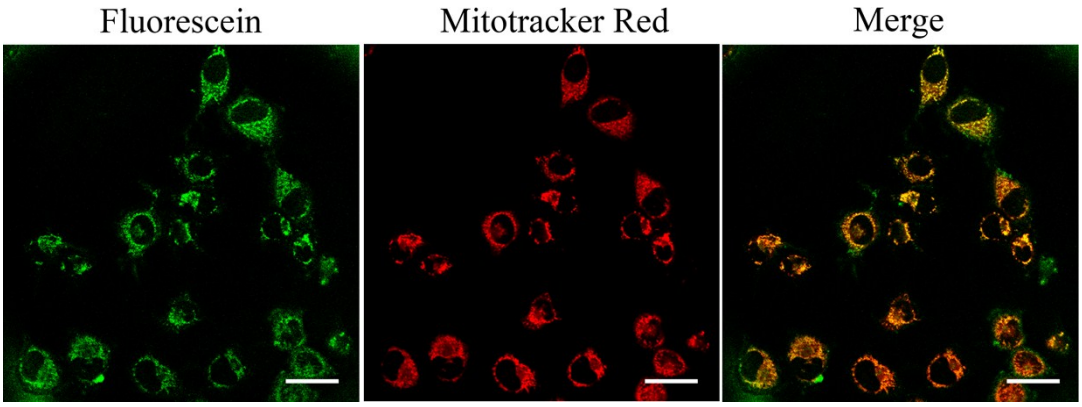

Fig. S15 The CLSM images of intracellular localization of TPP-Flu nanoparticles in HeLa cells after treatment. Scale bars are 20 μm.

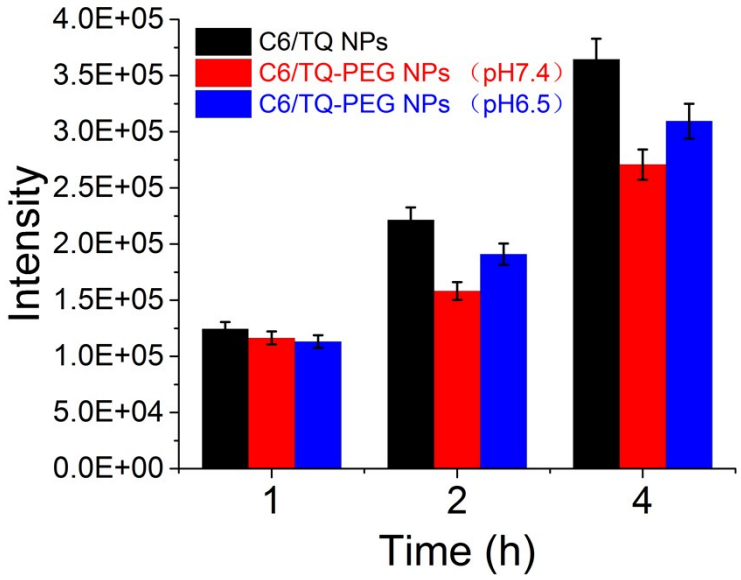

Fig. S14 The cellular uptake of the C6/TQ NPs, C6/TQ-PEG NPs and dePEGylation of C6/TQ-PEG NPs in the pH 6.5.

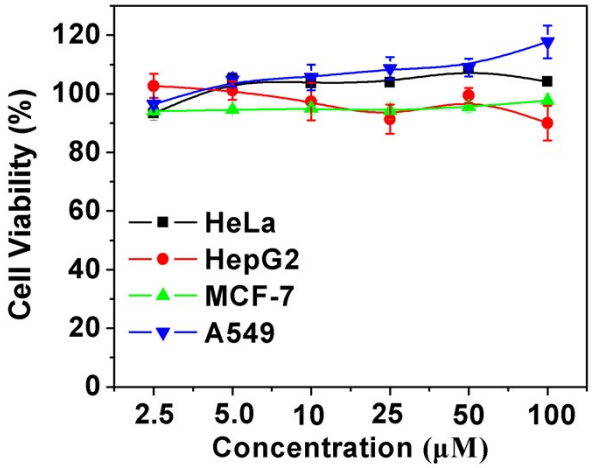

Fig. S17 *In vitro* cytotoxicity of TF NPs to HeLa cells, HepG2 cell, MCF-7 cells and A549 cells determined by MTT assay. The data are presented as average ± standard error (n= 3).

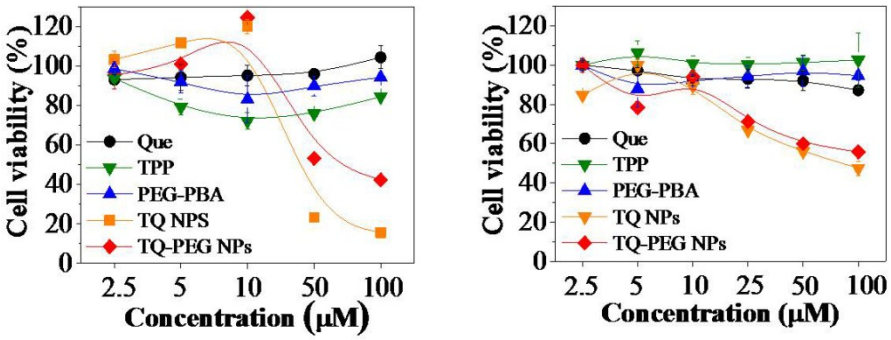

Fig. S18 *In vitro* cytotoxicity of various formulations to MCF-7 and A549 cells determined by MTT assay. The data are presented as average ± standard error (n= 3).

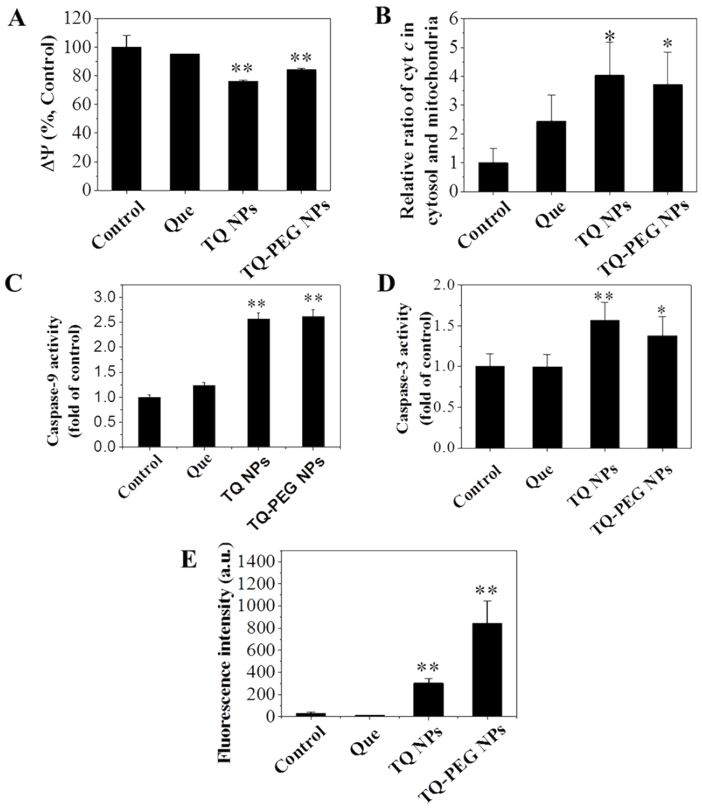

Fig. S19 Activation of the mitochondria-mediated apoptosis pathway. (A) Mitochondrial membrane potential of HeLa cells after treatment with different formulations. (B) Cyt *c* ratio in cytoplasm and mitochondria was determined by ELISA. The activation of caspase-9 (C) and caspase-3 (D) caused by various formulations. (E) Intracellular ROS level after treatment with different formulations in HeLa cells (n = 3, * $p < 0.05$, **$p < 0.01$).

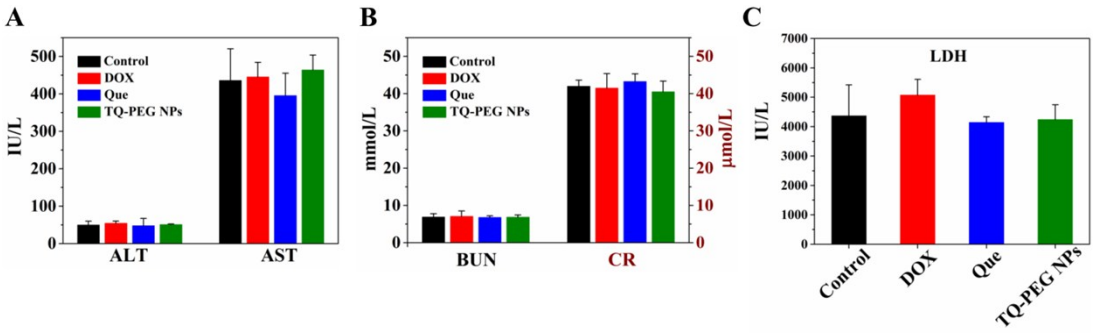

Fig. S20 Blood biochemistry data of mice, including changes of (A) liver function markers: ALT and AST, (B) kidney function markers: BUN and CR, and (C) heart function marker: LDH. No significant difference was observed between each group. The data are presented as average ± standard error (n= 4).

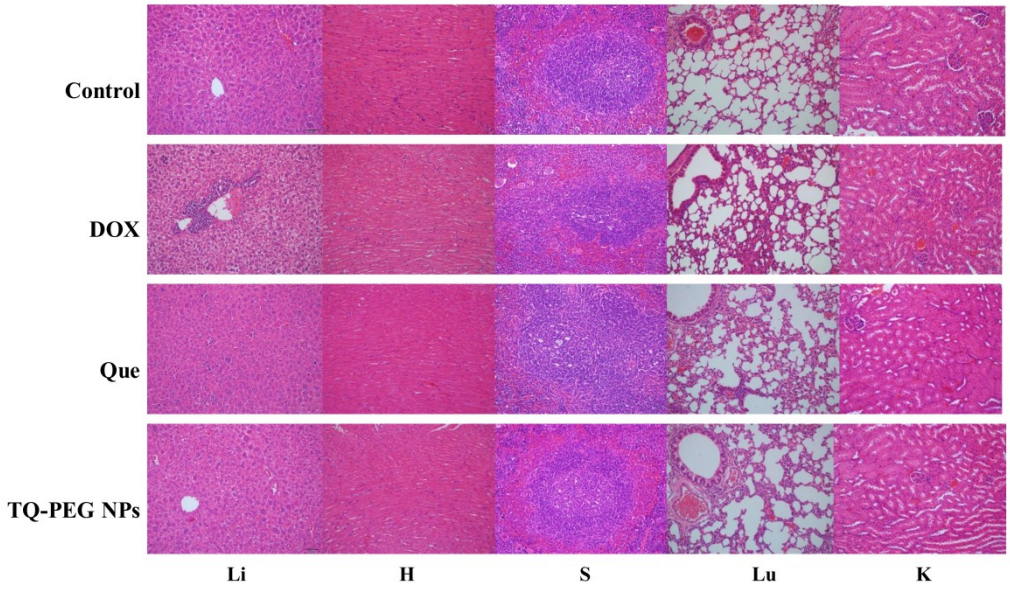

Fig. S21 Representative images of paraffin-embedded major organs sections of different groups after H&E staining. Scale bar is 50 μm.

Reference

1 Q. Hu, M. Gao, G. Feng, B. Liu, *Angew. Chem. Int. Ed.,* 2014, **53**, 14225.

2 S. Chalmers, S. T. Caldwell, C. Quin, T. A. Prime, A. M. James, A. G. Cairns, M. P. Murphy, J. G. McCarron, R. C. Hartley, *J. Am. Chem. Soc.,* 2012, **134**, 758.

3 A. Mattarei, L. Biasutto, E. Marotta, U. De Marchi, N. Sassi, S. Garbisa, M. Zoratti, C. A. *Chembiochem,* 2008, **9**, 2633.

4 E. E. Nekongo, V. V. Popik, *J. Org. Chem.,* 2014, **79**, 7665.

5 J. Yune, K. Molvinger, F. Quignard, *Catal. Today,* 2008, **138**, 104.

6 A. Adamczyk-Woźniak, M. K. Cyrański, B.T. Frączak, A. Lewandowska, I. D. Madura, A. Sporzyński, *Tetrahedron,* 2012, **68**, 3761.

7 P. Huang, D. Wang, Y. Su, W. Huang, Y. Zhou, D. Cui, X. Zhu, D. Yan, *J. Am. Chem. Soc.,* 2014, **136**, 11748.

8 J. E. Chung, S. Tan, S. J. Gao, N. Yongvongsoontorn, S.H. Kim, J. H. Lee, H. S. Choi, H. Yano, L. Zhuo, M. Kurisawa J. Y. Ying, *Nat. Nanotechnol.,* 2014, **9**, 907.

9 J. Su, F. Chen, V. L. Cryns, P. B. Messersmith, *J. Am. Chem. Soc.,* 2011, **133**, 11850.

10 H. L. Jiang, Y. K. Kim, R. Arote, J. W. Nah, M. H. Cho, Y. J. Choi, T. Akaike, C. S. Cho, *J. Controlled Release,* 2007, **117**, 273.

11 F. Z. Wang, Z. S. Xie, L. Xing, B. F. Zhang, J. L. Zhang, P. F. Cui, J. B. Qiao, K. Shi, C. S. Cho, M. H. Cho, X. Xu, P. ,Li, H. L. Jiang, *Biomaterials,* **2015**, 73, 149.

12 R. I. El-Gogary, N. Rubio, J. T. Wang, W. T. Al-Jamal, M. Bourgognon, H. Kafa, M. Naeem, R. Klippstein, V. Abbate, F. Leroux, S. Bals, T. G. Van, A. O. Kamel, G. A. Awad, N. D. Mortada, K. T. Al-Jamal, *ACS nano,* 2014, **8**, 1384.

13 F. Puoci, C.Morelli, G. Cirillo, M. Curcio, O. I. Parisi, P. Maris, D. Sisci, N. Picci, *Anticancer Res.,* 2012, **32**, 2843.